  Bull. Chem. Soc. Jpn., 60, 1469—1479 (1987)

Aggregate Morphology of Peptide Lipids Having Hydroxyl Groups: Molecular Basis for Formation of Inverted Hexagonal, Inverted Cubic, Bilayer, and Micellar Phases

Yukito MURAKAMI,* Jun-ichi KIKUCHI, Toshihiko TAKAKI, and Katsuya UCHIMURA
Department of Organic Synthesis, Faculty of Engineering, Kyushu University, Hakozaki, Higashi-ku, Fukuoka 812
(Received October 24, 1986)

Three types of peptide lipids having different numbers of hydroxyl groups in their head moieties, (HO)C_5-Ala2C_n, QC_5Ala2C_n, and Q_2LysC_5Ala2C_n (n=14, 16), were prepared, and their morphological behavior was investigated by various physical techniques: negative staining and freeze-fracture electron microscopy, low-angle X-ray diffraction, selected area electron diffraction, fluorescence polarization spectroscopy, and differential scanning calorimetry. QC_5Ala2C_n, having four hydroxyl groups in the head moiety, underwent aggregation in the aqueous dispersion state to afford the nonbilayer phase, which was constituted with highly developed globular domains with face-centered cubic (C_{II}) lattice, above the phase transition temperature (T_m). This C_{II} phase was transformed into the bilayer one below T_m. On the other hand, Q_2LysC_5Ala2C_n, having eight hydroxyl groups in the head moiety, formed bilayer aggregates in a whole temperature range, above and below T_m. Deprotonation of the hydroxyl groups of QC_5Ala2C_n and Q_2LysC_5Ala2C_n resulted in morphological changes to afford the bilayer and micellar phases, respectively. Two-component lipid systems composed of (HO)C_5Ala2C_{14} and Q_2LysC_5Ala2C_{14} at appropriate molar ratios afforded the inverted hexagonal (H_{II}) phase in the aqueous dispersion state; the first example of the H_{II} phase formed with artificial double-chain amphiphiles. The aggregate morphology was discussed on the basis of the critical packing mode of lipid molecules.

Extensive studies on structures and functions of biomembranes gave an impetus to rapid growth of *membrane mimetic chemistry*.[1] While synthetic lipids having a wide variety of molecular structures have been demonstrated to afford bilayer aggregates, structural limitations of such lipids in morphological behavior have not been unveiled up to the present time. Nonbilayer structures, such as inverted hexagonal and inverted cubic ones, have often been observed with natural lipid systems,[2] and some useful concepts have been proposed to explain the molecular basis for the formation of such aggregates.[3,4] However, feedback of these concepts to the development of artificial lipids requires the guidepost for molecular design of lipids, which adopt desired aggregate structures, and such attempts have encountered some difficulties.[5] In other words, appropriate structural modifications must be systematically exercised in designing artificial lipids, so that changes in their morphological behavior are significantly amplified. The *peptide lipids* are suitable candidates for such purposes, since amino acid residues involved in aggregates of these lipids form the tight hydrogen-belt domain which acts to separate two intramembrane domains, the surface domain composed of polar head moieties and the hydrophobic interior domain formed with double-chain segments, so that direct structural interactions between the latter two domains tend to be minimized.[6] Thus, only the size of double-chain segments of the lipid molecules primarily controls the phase transition behavior.[6c,7] On these grounds, we can exactly evaluate the effects of structural modifications of lipid molecules on aggregate morphology. In the present work, we investigated the aggregate morphology of individual and mixed lipid systems of the following three types of peptide lipids having different numbers of hydroxyl groups in their head moieties; (HO)C_5-Ala2C_n, QC_5Ala2C_n, and Q_2LysC_5Ala2C_n (n=14, 16). Four different types of aggregate morphology, inverted hexagonal, inverted cubic, bilayer, and micellar phases, were systematically created for the first time with these artificial lipids by controlling the packing mode of lipid molecules in the aggregate state.

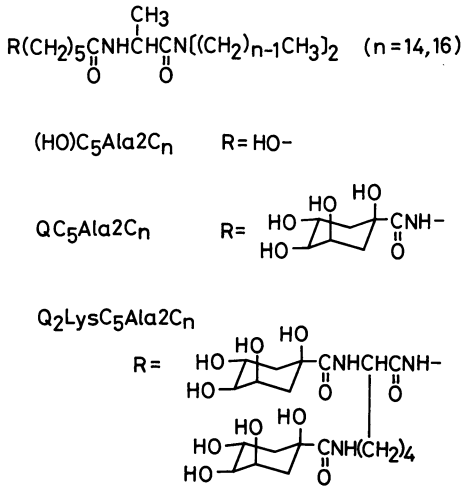

Experimental

Materials. 1,6-Diphenyl-1,3,5-hexatriene (DPH) was obtained from Nakarai Chemicals as a guaranteed reagent and used without further purification. Trisodium 8-hydroxy-1,3,6-pyrenetrisulfonate (pyranine) was purchased from Tokyo Kasei Kogyo Co. and purified after the method reported by Kano and Fendler.[8] Hexadecyltrimethylammonium bromide (CTAB) from Nakarai Chemicals was recrystallized from ethanol, mp 237—239 °C (decomp). Preparation of nonionic peptide lipids having the 1,3,4,5-tetrahydroxy-[1*R*-(1α,3α,4α,5β)]cyclohexylcarbonyl (quinoyl) moiety has been reported previously: *N,N*-dihexadecyl-N^{α}-[6-(quinoylamino)hexanoyl]-L-alaninamide (QC_5Ala2C_{16})[7] and *N,N*-ditetradecyl-N^{α}-[6-(quinoylamino)hexanoyl]-L-alaninamide

(QC_5Ala2C_{14}).[9]

***N,N*-Dihexadecyl-N^{α}-(6-hydroxyhexanoyl)-L-alaninamide [(HO)C_5Ala2C_{16}].** A mixture of *N,N*-dihexadecyl-N^{α}-(6-bromohexanoyl)-L-alaninamide[7] (1.0 g, 1.6 mmol), formamide (2.5 g, 86 mmol), and water (60 mg, 3.2 mmol) was stirred for 3 h at 140—150 °C and cooled to room temperature. Water (4 mL) was added to the mixture, which was subsequently extracted with dichloromethane (3×10 mL). The solvent was removed in vacuo, and the residue was dissolved in ethanol (20 mL). Aqueous NaOH (2 mol dm^{-3}, 3 mL) was added to the ethanol solution, and the resulting solution was refluxed for 3 h. After addition of water (10 mL), the mixture was acidified with hydrochloric acid and extracted with chloroform (3×15 mL). The extract was washed with water, dried over sodium sulfate, and evaporated to dryness in vacuo. The residue was purified by gel-filtration chromatography on a column of Sephadex LH-20 with methanol as an eluant: a colorless solid, yield 110 mg (11%); mp 44.8—45.2 °C; IR (KBr) 3440 (OH), 3280 (NH), 2920 and 2845 (CH), and 1635 cm^{-1} (C=O); ^1H NMR ($CDCl_3$, Me_4Si) δ=0.87 [6H, t, $(CH_2)_{15}C\underline{H}_3$], 1.25 [65H, m, $CH_2(C\underline{H}_2)_{14}CH_3$, $CH(C\underline{H}_3)$, and $HOCH_2(C\underline{H}_2)_3CH_2$], 2.20 [2H, t, $HO(CH_2)_4C\underline{H}_2$], 3.2 [4H, m, $C\underline{H}_2(CH_2)_{14}CH_3$], 3.60 [2H, t, $HOC\underline{H}_2$], 4.83 [1H, m, $C\underline{H}(CH_3)$], and 6.60 [1H, d, CONH].

Found: C, 74.55; H, 12.50; N, 4.33%. Calcd for $C_{41}H_{82}N_2O_3 \cdot 1/2\ H_2O$: C, 74.60; H, 12.67; N, 4.24%.

***N,N*-Ditetradecyl-N^{α}-(6-hydroxyhexanoyl)-L-alaninamide [(HO)C_5Ala2C_{14}].** This was prepared from *N,N*-ditetradecyl-N^{α}-(6-bromohexanoyl)-L-alaninamide[7] in a manner similar to that stated above: a colorless solid, yield 18%; mp 48.5—49.0 °C; IR (KBr) 3440 (OH), 3280 (NH), 2920 and 2845 (CH), and 1635 cm^{-1} (C=O); ^1H NMR ($CDCl_3$, Me_4Si) δ=0.88 [6H, t, $(CH_2)_{13}C\underline{H}_3$], 1.25 [57H, m, $CH_2(C\underline{H}_2)_{12}CH_3$, $CH(C\underline{H}_3)$, and $HOCH_2(C\underline{H}_2)_3CH_2$], 2.20 [2H, t, $HO(CH_2)_4C\underline{H}_2$], 3.2 [4H, m, $C\underline{H}_2(CH_2)_{12}CH_3$], 3.59 [2H, t, $HOC\underline{H}_2$], 4.84 [1H, m, $C\underline{H}(CH_3)$], and 6.60 [1H, d, CONH].

Found: C, 74.34; H, 12.39; N, 4.75%. Calcd for $C_{37}H_{74}N_2O_3$: C, 74.69; H, 12.54; N, 4.71%.

***N,N*-Dihexadecyl-N^{α}-[6-[[N^{α},N^{ε}-bis(*t*-butoxycarbonyl)-L-lysyl]amino]hexanoyl]-L-alaninamide [(Boc)$_2$LysC_5Ala2C_{16}].** Trifluoroacetic acid (25 g, 220 mmol) was added to a dry dichloromethane solution (20 mL) of *N,N*-dihexadecyl-N^{α}-[6-(*t*-butoxycarbonylamino)hexanoyl]-L-alaninamide[7] (5.0 g, 6.7 mmol), and the mixture was stirred for 4.5 h at room temperature. An excess amount of trifluoroacetic acid and the solvent were evaporated off in vacuo. The residue was dissolved in chloroform (50 mL) and then washed with 5% aqueous sodium hydrogencarbonate (3×30 mL). After being dried over sodium sulfate, the solution was evaporated to dryness in vacuo to give a pale yellow solid (3.0 g). Elimination of the *t*-butoxycarbonyl group was confirmed by IR and ^1H NMR spectroscopy. Dicyclohexylcarbodiimide (0.93 g, 4.5 mmol) was added to a dry dichloromethane solution (20 mL) of the N^{α},N^{ε}-bis(*t*-butoxycarbonyl)-L-lysine dicyclohexylamine salt (2.3 g, 4.5 mmol) and *p*-toluenesulfonic acid (0.77 g, 4.5 mmol) at 0 °C. After the mixture being stirred for 15 min at 0 °C, a dry dichloromethane solution (10 mL) of the amine was added to it at the same temperature. The mixture was stirred for 3 h at 0 °C and overnight at room temperature. The resulting precipitate (*N,N'*-dicyclohexylurea) was removed by filtration, the filtrate was evaporated to dryness in vacuo, and the residue was dissolved in ethyl acetate (100 mL). The ethyl acetate solution was then washed with 10% aqueous citric acid (2×50 mL), water (50 mL), 4% aqueous sodium hydrogencarbonate (2×50 mL), and water (50 mL) in this sequence. After being dried over sodium sulfate, the solution was evaporated to dryness in vacuo. The residue was chromatographed on a column of silica gel (Wako Gel C-100) with chloroform as an eluant: a pale yellow solid, yield 1.7 g (22%); IR (KBr) 3320 (NH), 2920 and 2850 (CH), and 1770 and 1660 cm^{-1} (C=O); ^1H NMR ($CDCl_3$, Me_4Si) δ=0.87 [6H, t, $(CH_2)_{15}C\underline{H}_3$], 1.25 [71H, m, $CH_2(C\underline{H}_2)_{14}CH_3$, $CH(C\underline{H}_3)$, $CONHCH_2(C\underline{H}_2)_3CH$, and $CONHCH_2(C\underline{H}_2)_3CH_2$], 1.42 [18H, s, $OC(CH_3)_3$], 2.3 [2H, m, $CONH(CH_2)_4C\underline{H}_2$], 3.14 [8H, m, $CONHC\underline{H}_2$ and $C\underline{H}_2$-$(CH_2)_{14}CH_3$], 4.27 [3H, m, $C\underline{H}(CH_2)_3$ and $CONHC\underline{H}_2$], 4.80 [1H, m, $C\underline{H}(CH_3)$], 5.12 [1H, d, $OCONH\underline{C}H$], and 7.60 [1H, d, $CONH\underline{C}H$].

***N,N*-Dihexadecyl-N^{α}-[6-[[N^{α},N^{ε}-bis(tetraacetylquinoyl)-L-lysyl]amino]hexanoyl]-L-alaninamide [(AcQ)$_2$LysC_5Ala2C_{16}].** Trifluoroacetic acid (25 g, 220 mmol) was added to a dry dichloromethane solution (20 mL) of (Boc)$_2$LysC_5Ala2C_{16} (1.1 g, 1.1 mmol), and the mixture was stirred for 2 h at room temperature. Evaporation of an excess amount of trifluoroacetic acid and the solvent gave a pale yellow oil (1.2 g). Elimination of the *t*-butoxycarbonyl group was confirmed by ^1H NMR spectroscopy. The amine was dissolved in dry dichloromethane (20 mL), and the solution was cooled to 0 °C. Triethylamine (2.3 g, 22 mmol) was added to the solution, and then (−)-tetraacetylquinoyl chloride[10] (1.7 g, 4.5 mmol) dissolved in dry dichloromethane (20 mL) was added dropwise to the mixture at 0 °C with stirring. The resulting mixture was stirred for 1 h at 0 °C and for 2 h at room temperature, and then dichloromethane (100 mL) was added to it. The mixture was washed with saturated aqueous sodium chloride (2×50 mL), 5% aqueous citric acid (2×50 mL), saturated aqueous sodium chloride (2×50 mL), 5% aqueous sodium hydrogencarbonate (2×50 mL), and saturated aqueous sodium chloride (2×50 mL) in this sequence. After being dried over sodium sulfate, the solution was evaporated to dryness in vacuo. The residue was chromatographed on a column of silica gel (Wako Gel C-100) with ethyl acetate as an eluant. The product was further purified by gel-filtration chromatography on a column of Sephadex LH-20 with methanol as an eluant: a colorless solid, yield 0.32 g (20%); mp 75.0—76.5 °C; IR (KBr) 2920 and 2850 (CH), and 1740 and 1650 cm^{-1} (C=O).

***N,N*-Dihexadecyl-N^{α}-[6-[(N^{α},N^{ε}-diquinoyl-L-lysyl)amino]-hexanoyl]-L-alaninamide [Q_2LysC_5Ala2C_{16}].** After addition of hydrazine monohydrate (700 mg, 14 mmol) to a solution of (AcQ)$_2$LysC_5Ala2C_{16} (270 mg, 0.19 mmol) in 85% aqueous ethanol (3 mL), the mixture was refluxed for 1 h, cooled to room temperature, and poured into cold water (20 mL). Chloroform (30 mL) was added to the mixture, and the organic layer was separated by centrifugation. After being dried over sodium sulfate, the organic layer was evaporated to dryness in vacuo. The residue was purified by gel-filtration chromatography on a column of Sephadex LH-20 with methanol as an eluant: a colorless solid, yield 120 mg (59%); final mp 227 °C; IR (KBr) 3350 (OH), 2920 and 2850 (CH), and 1640 cm^{-1} (C=O).

Found: C, 64.07; H, 10.26; N, 6.20%. Calcd for $C_{61}H_{115}N_5O_{13} \cdot H_2O$: C, 64.01; H, 10.30, N, 6.12%.

***N,N*-Ditetradecyl-N^{α}-[6-[(N^{α},N^{ε}-diquinoyl-L-lysyl)amino]-hexanoyl]-L-alaninamide [Q_2LysC_5Ala2C_{14}].** This was prepared from *N,N*-ditetradecyl-N^{α}-[6-(*t*-butoxycarbonyl-

amino)hexanoyl]-L-alaninamide[7] in a manner similar to that stated above: a colorless solid; final mp 173 °C; IR (KBr) 3350 (OH), 2920 and 2850 (CH), and 1640 cm^{-1} (C=O).

Found: C, 62.93; H, 10.32; N, 6.45%. Calcd for $C_{57}H_{107}N_5O_{13}\cdot H_2O$: C, 62.89; H, 10.09; N, 6.43%.

Analyses and Measurements. Elemental analyses were performed at the Microanalysis Center of Kyushu University. Melting points were measured with a Yanagimoto MP-S1 apparatus (hot-plate type). ^1H NMR spectra were taken on a Hitachi R-24B spectrometer. IR spectra were recorded on a JASCO IR-810 spectrophotometer. pH Measurements were carried out with a Beckman Φ71 pH meter equipped with a Beckman 39505 combined electrode after calibration with a combination of appropriate standard aqueous buffers. A JASCO UVIDEC-100 UV spectrophotometer was used as a detector for gel-filtration chromatography. Fluorescence spectra were recorded on a Hitachi 650-60 spectrofluorometer. A Daini Seikosha SSC-560U calorimeter was used for differential scanning calorimetry (DSC). The phase-transition temperature (T_m, temperature at a peak maximum of DSC thermogram) and the enthalpy change for phase transition (ΔH) were determined in a manner as reported previously.[7]

Electron micrographs were taken on a JEOL JEM-2000FX electron microscope installed at the Research Laboratory for High Voltage Electron Microscopy of Kyushu University. Negatively stained and freeze-fractured samples for the measurements were prepared in a manner as described previously.[7] Selected area electron diffraction measurements were carried out by using the same electron microscope, electron wavelength being adjusted at 100 kV (λ=0.037 Å). The camera length (2870 mm) was calibrated on the basis of diffractions from (111) and (200) planes of the face-centered cubic lattice of single crystalline gold.

The fluorescence polarization measurements were carried out on a Union Giken FS-501A fluorescence polarization spectrophotometer equipped with a Sord microcomputer M200 Mark II; emission at 450 nm originated from DPH was monitored upon excitation at 358 nm with a slit width of 3.5 nm for both excitation and emission sides. The steady-state fluorescence anisotropy (r_S) was calculated by Eq. 1, where I is the fluorescence intensity, and the subscripts v and h refer to the orientations, vertical and horizontal, respectively, for the excitation and analyzer polarizers in this sequence. C_f is the grating correction factor, given by I_{hv}/I_{hh}.

$$r_S = (I_{vv} - C_f I_{vh})/(I_{vv} + 2C_f I_{vh}), \quad (1)$$

The nickel-filtered Cu $K\alpha$ radiation (λ=1.542 Å) from a Rigaku Rotaflex RU-200 X-ray generator was used for X-ray diffraction measurements. Each sample was sealed up in a specimen holder equipped with mica windows, and a low-angle diffraction pattern was recorded on a Fuji X-ray film 150; a sample-film distance being set at 200 mm.

Results and Discussion

Molecular Design of Nonionic Peptide Lipids. Ionic peptide lipids having an α-amino acid residue interposed between a polar head moiety and a hydrophobic double-chain segment generally form bilayer aggregates in an aqueous dispersion state.[6] On the other hand, we have recently found that nonlamellar aggregates appear in the aqueous dispersions of cationic and anionic lipids, *N,N*-dialkyl-*N*$^{\alpha}$-[6-(trimethylammonio)hexanoyl]-L-alaninamide bromide [N^+C_5-Ala2C_n] and sodium *N,N*-dialkyl-*N*$^{\alpha}$-(6-sulfonatohexanoyl)-L-alaninamide [(SO_3^-)C_5Ala2C_n], respectively, mixed at the 1:1 molar ratio above the phase-transition temperature (T_m).[11] This nonlamellar phase is

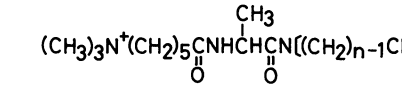

N^+C_5Ala2C_n (n= 8, 10, 12, 14, 16, 18)

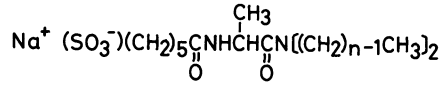

(SO_3^-)C_5Ala2C_n (n = 14, 16)

referred to the inverted cubic (C_{II}) one composed of three-dimensional network of globular aggregates with small internal aqueous compartments.[12] The following two effects control the packing mode of lipid molecules to adopt the C_{II} phase in aqueous media: (i) intramembrane electrostatic interactions between cationic and anionic head moieties to form highly developed ion-pair clusters in the membrane surface, and (ii) recovery of the rotational and bending motions of hydrophobic double-chain segments above T_m. As a result, these lipid molecules are allowed to retain the *inverted truncated cone* shape[4a] in their aggregates above T_m, and the critical packing mode under such conditions favors the formation of inverted micellar aggregates. We have also found that the nonlamellar phase was formed with nonionic peptide lipids having the quinoyl moiety, QC_5Ala2C_n, through the hydrogen-bonding interaction among the polar head moieties. These observations imply that the peptide lipids tend to construct various aggregate structures, which have been demonstrated so far with naturally occurring lipid systems, in aqueous media by manipulating steric bulkiness of their polar head moieties so that specific packing modes are attained in their aggregates.

A useful concept has been proposed on the self-assembling behavior of lipid molecules in dilute aqueous solutions, based on the critical packing parameter, v/a_0l_c, where v, a_0, and l_c are the hydrocarbon volume, the optimal surface area, and the critical chain length of lipid molecules, respectively.[4] The following guidepost for the formation of specific aggregate structures has been postulated on the basis of the dynamic packing mode: $v/a_0l_c < 1/3$ for spherical micelles, $1/3 < v/a_0l_c < 1/2$ for cylindrical micelles, $1/2 < v/a_0l_c < 1$ for bilayers, and $v/a_0l_c > 1$ for inverted micelles.[4] However, there are few successful explanations to distinguish between structural factors for the formation of the two kinds of nonlamellar phases; a hexagonally

packed array of inverted cylindrical micelles (H_{II} phase), and a closely packed cubic array of inverted spherical micelles (C_{II} phase).[13] Recently, Verkleij mentioned in his review article that lipidic particles are found in a variety of lipid mixtures and in total lipid extracts under physiological conditions in excess water, and that lipidic particles are only found in mixed systems of natural lipids, in which one component or more of the lipids prefer to adopt the H_{II} phase in their individual states.[2a] Since the C_{II} phase is considered to be the principal morphology pertaining to lipidic particles, the C_{II} aggregate is granted to be the intermediary form lying between bilayer and H_{II} ones. Thus, the critical packing parameter for the H_{II} forming lipid seems to be larger than that for the C_{II} forming lipid.

As for the peptide lipids, the critical packing parameter is primarily controlled by the a_0 value if only the polar head moiety undergoes structural variation and the rest of the molecule remains the same. As one of such purposive series of lipid molecules, we prepared three types of nonionic peptide lipids having various numbers of hydroxyl groups in their head moieties; (HO)C_5Ala2C_n, QC_5Ala2C_n, and Q_2LysC_5-Ala2C_n (n=14, 16). The CPK molecular models of these lipids are shown in Fig. 1. Since the four hydroxyl groups of the quinoyl moiety are located on one side of the cyclohexane ring with chair-type conformation, the head moieties of QC_5Ala2C_n and Q_2LysC_5Ala2C_n seem to hold configurations paralled to the membrane surface. In addition, the extent of solvation of the head moieties of the present lipids mainly depends on a number of the hydroxyl groups in the presence of excess water. Thus, the a_0 value for the present peptide lipids decreases in the following order: Q_2LysC_5Ala2C_n > QC_5Ala2C_n > (HO)C_5Ala2C_n. Now, correlations between aggregate morphology and lipid structure are described below on the basis of the critical packing concept.

Inverted Cubic Phase. Recently, we have found that QC_5Ala2C_n having four hydroxyl groups in the head moiety form nonlamellar aggregates in the aqueous dispersion state by means of negative staining electron microscopy.[9] The low-angle X-ray diffraction technique was applied to these aggregates in this work. Four diffractions with the spacing ratio, $1:\sqrt{3}/2:\sqrt{3}/\sqrt{8}:1/2$, were observed for QC_5Ala2C_n (n=14, 16) at pH 7 above T_m (Table 1). This spacing ratio is in conformity with diffractions from (111), (200), (220), and (222) planes of the face-centered cubic (fcc) lattice with lattice constant a (Fig. 2). We have obtained similar diffraction patterns for aggregates formed with equimolar mixtures of cationic and anionic lipids.[12] It has been claimed that an apparent cubic phase observed in the 1-oleoylglycerol-water system actually consists of a lipid bilayer forming a tetrahedral periodic minimal surface which separates two water channel networks.[14] The existence of such continuous

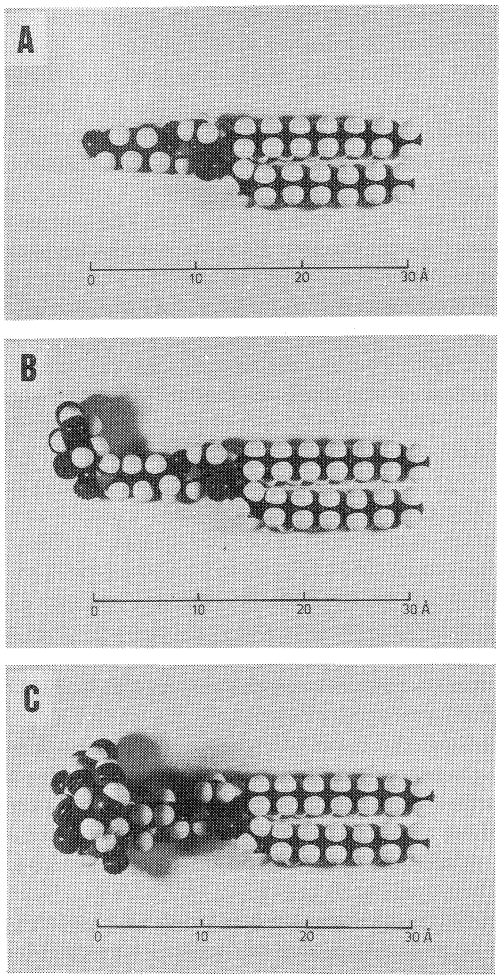

Fig. 1. CPK molecular models of (HO)C_5Ala2C_{14} (A), QC_5Ala2C_{14} (B), Q_2LysC_5Ala2C_{14} (C).

water channels in our peptide lipid systems, however, can be ruled out in the light of the electron microscopic measurements.[9,11,12] The (111) plane of the fcc lattice is the closest packed one, and the distance between the nearest neighbors in the plane ($a/\sqrt{2}$) is referred to the repeating distance of internal aqueous compartments. When the weight fraction of QC_5-Ala2C_{14} in water was increased from 0.22 to 0.28, the $a/\sqrt{2}$ value was reduced by 9 Å. In addition, the $a/\sqrt{2}$ value as observed by negative staining electron microscopy, for which water was completely removed during the sample preparation, was 70 Å.[9] Such large dependence of the $a/\sqrt{2}$ value on the lipid concentration seems to be originated from the fact that the hydrogen-bonding interaction among polar head moieties of the lipid molecules predominantly controls the critical packing mode to give thermodynamically stable aggregates and water molecules solvated onto the head moieties also take part in the hydrogen-bonding interaction. In dilute aqueous solutions, on the other hand, the $a/\sqrt{2}$ value seems to approach to a limiting value (ca. 110 Å) in a manner as observed for an equimolar mixture of N^+C_5Ala2C_{14} and (SO_3^-)-C_5Ala2C_{14} by means of freeze-fracture electron micros-

Table 1. Low-Angle X-Ray Diffraction Data for QC_5Ala2C_n-Water Systems

n[a]	Lipid concn w/w%	pH	Temp °C	Spacing[b] Å	Relative intensity[c]	Lattice plane (hkl)	Lattice constant (a)/Å	$a/\sqrt{2}$ Å
14	22	7	25	83 (82)	s	(111)	142	100
				71 (71)	m	(200)		
				50 (50)	w	(220)		
				41 (41)	w	(222)		
14	28	7	25	75 (74)	s	(111)	128	91
				63 (64)	m	(200)		
				45 (45)	w	(220)		
				37 (37)	w	(222)		
14	22	14	25	59				
16	29	7	40	77 (77)	s	(111)	133	94
				66 (67)	m	(200)		
				47 (47)	w	(220)		
				38 (38)	w	(222)		
16	29	7	10	77	w			
				55	s			

a) A number of carbon atoms in the double-chain segment of QC_5Ala2C_n. b) Calculated values are given in parentheses. c) s, strong; m, medium; w, weak.

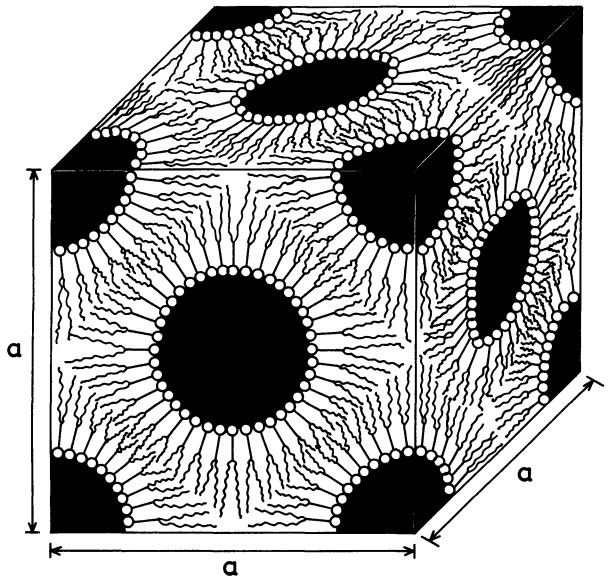

Fig. 2. Schematic representation of the inverted cubic phase formed with QC_5Ala2C_n; a, lattice constant.

copy.[11] It is noteworthy, however, that the $a/\sqrt{2}$ value is not so sensitively dependent on the lipid concentration for the cationic and anionic lipid system as observed for the QC_5Ala2C_{14} system in the light of observations by negative staining and freeze-fracture electron microscopy[11] and low-angle X-ray diffraction measurements.[12] The tight ion-pair cluster formed with cationic and anionic head moieties of the mixed lipid system seems to minimize hydration in the surface domain, while such an effect is not operative for QC_5Ala2C_n. These hydration effects must be reflected on the correlations between $a/\sqrt{2}$ and lipid concentration, and the $a/\sqrt{2}$ value is more strongly dependent on the lipid concentration in the case of the latter lipid system. The $a/\sqrt{2}$ value for the QC_5Ala2C_{16} aggregate (94 Å) is slightly larger than that for the QC_5Ala2C_{14} aggregate (91 Å) at a comparable concentration; mole fraction, 0.009.

Bilayer Phase. We have previously reported that the C_{II} phase formed with QC_5Ala2C_{14} was transformed into the bilayer phase upon deprotonation of the polar head moiety as confirmed by freeze-fracture electron microscopy, differential scanning calorimetry (DSC), and turbidity measurements.[7] This behavior was further evidenced by low-angle X-ray diffraction measurements in this work. As listed in Table 1, the diffractions from the C_{II} lattice at pH 7 completely disappeared at pH 14 to give a single diffraction with a spacing of 59 Å, which corresponds to the bilayer thickness evaluated by the CPK molecular model (Fig. 1B).

The diffraction patterns originating from the C_{II} phase formed with QC_5Ala2C_{16} disappeared below T_m even at pH 7 and were replaced with two diffractions (Table 1). The stronger diffraction with a spacing of 55 Å and the relatively weak one with a spacing of 77 Å presumably correspond to the thickness of the lipid bilayer and that of the bilayer plus water layer, respectively. Formation of the bilayer phase below T_m was also confirmed by negative staining electron microscopy applied to the specimen prepared at 5 °C. We have previously suspected that QC_5Ala2C_{16} would form the nonlamellar phase even below T_m on the basis of its smaller phase transition enthalpy and a lower value of steady-state fluorescence anisotropy for DPH embedded in the aggregate below T_m as compared with the corresponding values for bilayer-forming lipids having an analogous molecular structure.[7] Now, it is concluded that the C_{II} phase formed with QC_5Ala2C_{16} above T_m is transformed through phase transition into the bilayer phase accompanied with relatively loose packing of the hydrocarbon chains in comparison with those of bilayer-forming

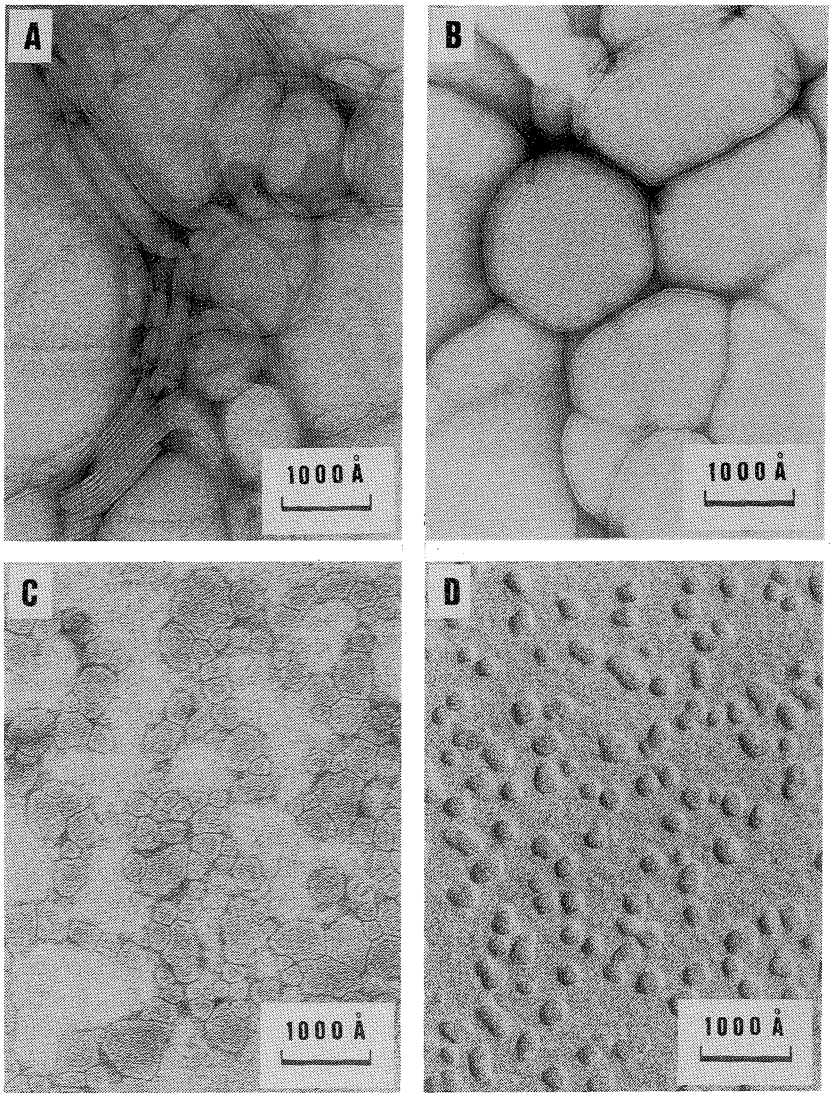

Fig. 3. Electron micrographs for $Q_2LysC_5Ala2C_n$: A, 5 mmol dm^{-3} aqueous dispersion of $Q_2LysC_5Ala2C_{16}$ negatively stained with uranyl acetate; B, 2.5 mmol dm^{-3} aqueous dispersion of $Q_2LysC_5Ala2C_{14}$ negatively stained with uranyl acetate; C, 2.5 mmol dm^{-3} aqueous solution of $Q_2LysC_5Ala2C_{14}$ sonicated for 2 min at 30 W, negatively stained with uranyl acetate; D, 1.5 mmol dm^{-3} aqueous solution of $Q_2LysC_5Ala2C_{14}$ sonicated for 3 min at 30 W, freeze-fractured.

ionic peptide lipids.

The phase transition parameters (T_m; enthalpy change, ΔH) for the aggegates of $Q_2LysC_5Ala2C_n$ having two quinoyl moieties are 1.7 °C and 17.1 kJ mol^{-1} for n=14 and 24.9 °C and 28.0 kJ mol^{-1} for n=16, respectively, at pH 7 as evaluated by DSC. These values are comparable to those observed for other bilayer aggregates having the same double-chain segments.[6c,7] The bilayer aggregates were formed both above and below T_m as observed by electron microscopy. As shown in Figs. 3A and 3B, multiwalled bilayer aggregates are observed in the specimens of $Q_2LysC_5Ala2C_{16}$ and $Q_2LysC_5Ala2C_{14}$, respectively, which were negatively stained at 20 °C in the aqueous dispersion state. Upon sonication of these dispersions with a probe-type sonicator, single-walled bilayer vesicles in the diameter range of 200—500 Å were obtained, as confirmed by negative staining and freeze-fracture electron microscopy (Figs. 3C and 3D). The steady-state fluorescence anisotropy (r_s) of DPH embedded in the $Q_2LysC_5Ala2C_{16}$ membrane is shown in Fig. 4 (curve A) as a function of temperature. The T_m value obtained from the inflection range (24.5 °C) is in good agreement with that evaluated by DSC. When homogeneous mixtures of QC_5Ala2C_n and $Q_2LysC_5Ala2C_n$ (n=14, 16) at the 1:1 and 2:1 molar ratios were dispersed in water, formation of multiwalled bilayer aggregates was detected by negative staining electron microscopy. Thus, it became apparent that transformation of the C_{II} phase formed with QC_5Ala2C_n above T_m into the bilayer phase can be achieved by the following perturbations to reduce the v/a_0l_c value: (i)

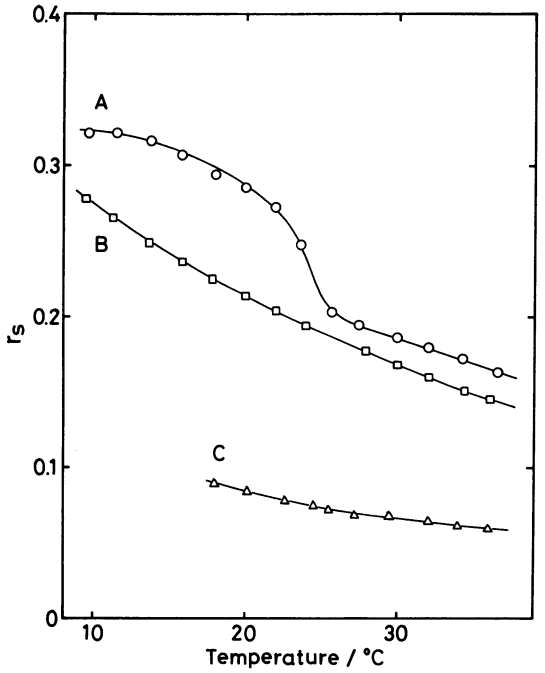

Fig. 4. Correlations of steady-state fluorescence anisotropy (r_S) with temperature for DPH (1.0×10^{-7} mol dm^{-3}) embedded in the following aggregates: A, 0.10 mmol dm^{-3} $Q_2LysC_5Ala2C_{16}$ at pH 7; B, 0.10 mmol dm^{-3} $Q_2LysC_5Ala2C_{16}$ at pH 14; C, 3.0 mmol dm^{-3} CTAB at pH 7.

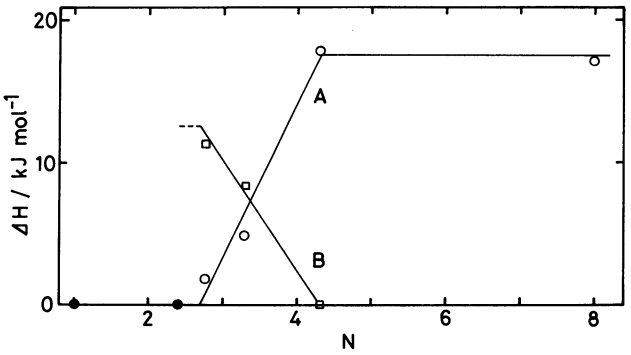

Fig. 5. Correlations of phase transition enthalpy (ΔH) with a number of hydroxyl groups per lipid molecule (N) for the aggregates formed with $(HO)C_5Ala2C_{14}$ and $Q_2LysC_5Ala2C_{14}$; total lipid concentration, 5.0 mmol dm^{-3}: A, for the phase transition peak at 1.8 °C; B, for the phase transition peak at 4.6 °C; closed circles for lipid mixtures which were not dispersed in water. The ΔH value is given for unit mol of the total lipid, regardless of morphology.

freezing of the rotational motion of the hydrophobic double-chain segment by a phase transition from the liquid-crystalline state to the gel state (decrease in v); (ii) a volume increase in the hydration shell around the polar head moiety of the lipid molecule upon deprotonation of the four hydroxyl groups (increase in a_0); and (iii) an increase in average bulkiness of the polar head moiety by incorporation of another bilayer-forming lipid (increase in a_0). In addition, it may be predicted that an increase in l_c, e.g. introduction of a longer hydrocarbon connector in between the quinoyl moiety and an amino acid residue, also causes a morphological change from C_{II} to bilayer.

Inverted Hexagonal Phase. As mentioned above, the H_{II} forming lipids may have v/a_0l_c values greater than those for the C_{II} forming lipids. We examined this criterion in this work by using the three types of nonionic peptide lipids. Since QC_5Ala2C_n forms the C_{II} phase above T_m, the individual or mixed lipid systems having a_0 values smaller than that of QC_5Ala2C_n are the candidates to form the H_{II} phase. Although accurate evaluation of the a_0 values for these peptide lipids is much difficult due to hydration of the polar head moieties, the effective bulkiness of these head moieties can be reasonably correlated with the average number of hydroxyl groups per lipid molecule (N): the N values for $(HO)C_5Ala2C_n$, QC_5Ala2C_n, and $Q_2LysC_5Ala2C_n$ are apparently 1, 4, and 8, respectively. $(HO)C_5Ala2C_n$ was not dispersed in water without coexisting lipid(s). When $(HO)C_5Ala2C_n$ and QC_5Ala2C_n were mixed at the 1 : 1, 1 : 2, and 1 : 4 molar ratios (N values are 2.5, 3.0, and 3.4, respectively), stable aqueous dispersions were not obtained even by prolonged vortex mixing.

Mixtures of $(HO)C_5Ala2C_{14}$ and $Q_2LysC_5Ala2C_{14}$ at the 1 : 1, 2 : 1, and 3 : 1 molar ratios (N values are 4.5, 3.3, and 2.8, respectively) were readily dispersed in water by vortex mixing, and turbidity of the aqueous dispersions remained unchanged at least over a week. The aggregates formed with $(HO)C_5Ala2C_{14}$ and $Q_2LysC_5Ala2C_{14}$ at the equimolar ratio showed a single phase transition at 1.8 °C, and the ΔH value was comparable to that observed for the bilayer aggregates formed with $Q_2LysC_5Ala2C_{14}$ alone (Fig. 5). The negatively stained electron micrograph showed the formation of multiwalled bilayer membranes. On the other hand, the DSC thermograms for the aggregates formed with $(HO)C_5Ala2C_{14}$ and $Q_2LysC_5Ala2C_{14}$ at the 2 : 1 and 3 : 1 molar ratios showed two phase transition peaks at 1.8 and 4.6 °C. The ΔH value for the latter peak increased as the N value was reduced, and the ΔH value for the former peak decreased concomitantly (Fig. 5). In the light of the correlations given in Fig. 5, the aggregate having T_m at 4.6 °C is referred to the H_{II} phase (above T_m) while that having T_m at 1.8 °C to the bilayer phase. In the negatively stained electron micrographs for these aggregates, three types of images, which are typical of the H_{II} phase, were observed: two kinds of striped patterns with different layer thickness and a network array of small internal aqueous compartments were observed in different areas of the specimen (Fig. 6). We evaluated these repeating distances by means of electron diffraction measurements applied to selected areas of the electron micrographs;[15] 52 and 31 Å of the repeating distances of layers (ratio, $\sqrt{3}$: 1) and 62 Å of the repeating dis-

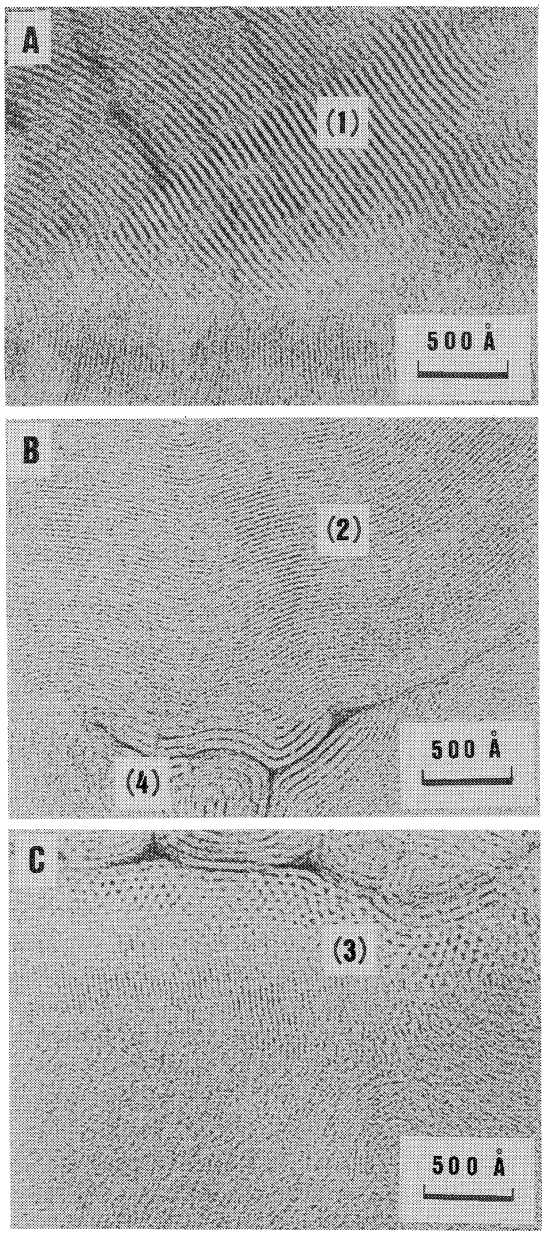

Fig. 6. Electron micrographs for a mixture of (HO)C_5Ala2C_{14} (3.33 mmol dm^{-3}) and Q_2LysC$_5$Ala2C_{14} (1.67 mmol dm^{-3}) in the aqueous dispersion state at room temperature, negatively stained with uranyl acetate. The images shown in A, B, and C were observed in different areas of the specimen. Numerals **1**, **2**, and **3** refer to three different cross sectional views of the H_{II} tubes, and **4** is attributed to the bilayer phase.

tance of aqueous compartments.[16] On these grounds, the aggregation status, which is referred to the H_{II} phase, is schematically illustrated in Fig. 7. The electron micrographic pattern, which presumably corresponds to the bilayer aggregate, was also observed in a limited area of the electron micrographs. However, it is rather difficult to distinguish between the image due to bilayer aggregates and that due to thicker layers of the H_{II} phase, since these show comparable layer thicknesses. The distinction between these aggregation states became possible by tilting the specimen in the electron microscope, as mentioned in our preliminary communication.[16] That is, the image and the corresponding electron diffraction pattern originating from one of the layers of the H_{II} phase were converted into those from the other type of layers by 30° rotation of the specimen (Fig. 8). The electron micrographic pattern showing a network array of internal aqueous compartments for the H_{II} phase resembles that for the C_{II} phase. However, the domain for the former phase is rather limited relative to that for the latter phase and surrounded by domains of the two types of layers attributable to the H_{II} phase. Fractions of the H_{II} phase in the overall aggregates were evaluated from the phase transition enthalpy; 0.7 and 0.9 for the (HO)C_5Ala2C_{14}-Q_2LysC_5Ala2C_{14} system at the molar ratios of 2 : 1 and 3 : 1, respectively. These lipid mixtures were not dispersed in water at the N value smaller than 2.4. However, the H_{II} phase seems to be exclusively obtained at the N value below 2.7 in the light of the correlations given in Fig. 5. The mixed lipid system composed of (HO)C_5Ala2C_{16} and Q_2LysC_5Ala2C_{16} did not give stable aqueous dispersions at the N value smaller than 4, so that the aggregate morphology was not critically characterized.

Micellar Phase. Multiple ionization of the polar head moiety of Q_2LysC_5Ala2C_n tends to expand the hydration shell around the quinoyl moieties to give an increase in a_0. As a result, the bilayer phase may be converted into the micellar one. The multiwalled bilayer aggregates formed with Q_2LysC_5Ala2C_n exhibited relatively large turbidity in aqueous media, presumably due to extended aggregation of the membranes, in comparison with those formed with cationic or anionic peptide lipids. Deprotonation of the hydroxyl groups of the lipids caused turbidity decrease above pH 13. We characterized the aggregates formed at pH 14 by means of DSC, gel-filtration treatments, and fluorescence polarization measurements. The phase transition peak observed for Q_2LysC_5Ala2C_n (n=14, 16) at pH 7 disappeared completely at pH 14 in the temperature range of 0—60 °C. Both dispersed and sonicated (with a probe-type sonicator at 30 W for 3 min) samples of Q_2LysC_5Ala2C_{16} at pH 14 were completely eluted at the void volume on a column of Sephadex G-50 with aqueous 1 mol dm^{-3} KOH as an eluant, as monitored by a UV detector at 254 nm. Then, we adopted experiments entrapping fluorescent probes into the aggregates. When DPH (1.0×10^{-5} mol dm^{-3}) was added to the aqueous dispersion of Q_2LysC_5Ala2C_{16} (1.0 mmol dm^{-3}), this hydrophobic probe was quantitatively incorporated into and remained in the aggregates even by gel-filtration treatments as confirmed by fluorescence spectroscopy. On the other hand, pyranine (1.0 mmol dm^{-3}) as a hydrophilic probe[8,17] was not incorporated at all into the aggregates of Q_2LysC_5Ala2C_{16} (1.0 mmol dm^{-3}) as confirmed by gel-filtration treatments at pH 14,

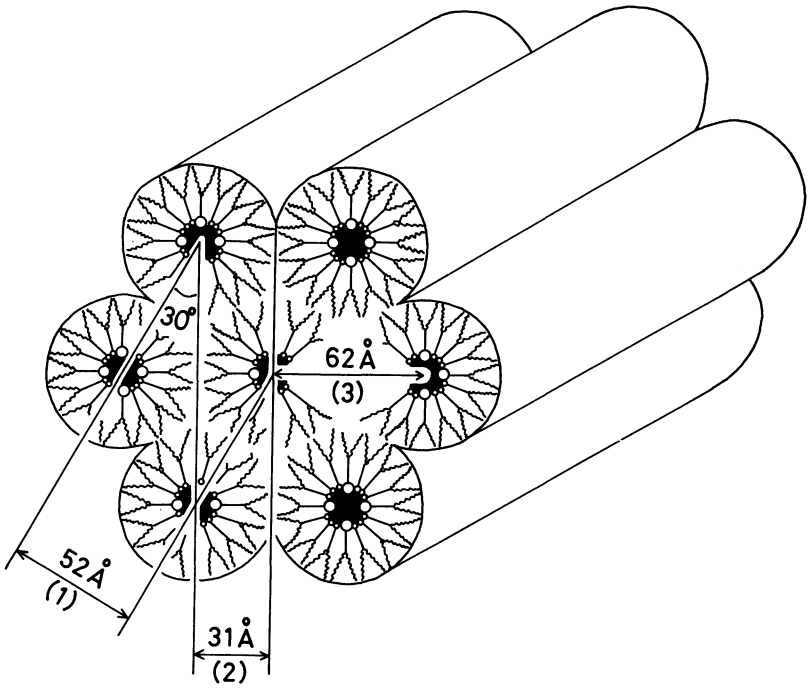

Fig. 7. Schematic representation of the inverted hexagonal phase formed with (HO)C_5Ala2C_{14} and Q_2LysC_5Ala2C_{14}; for numerals **1**, **2**, and **3**, refer to Fig. 6.

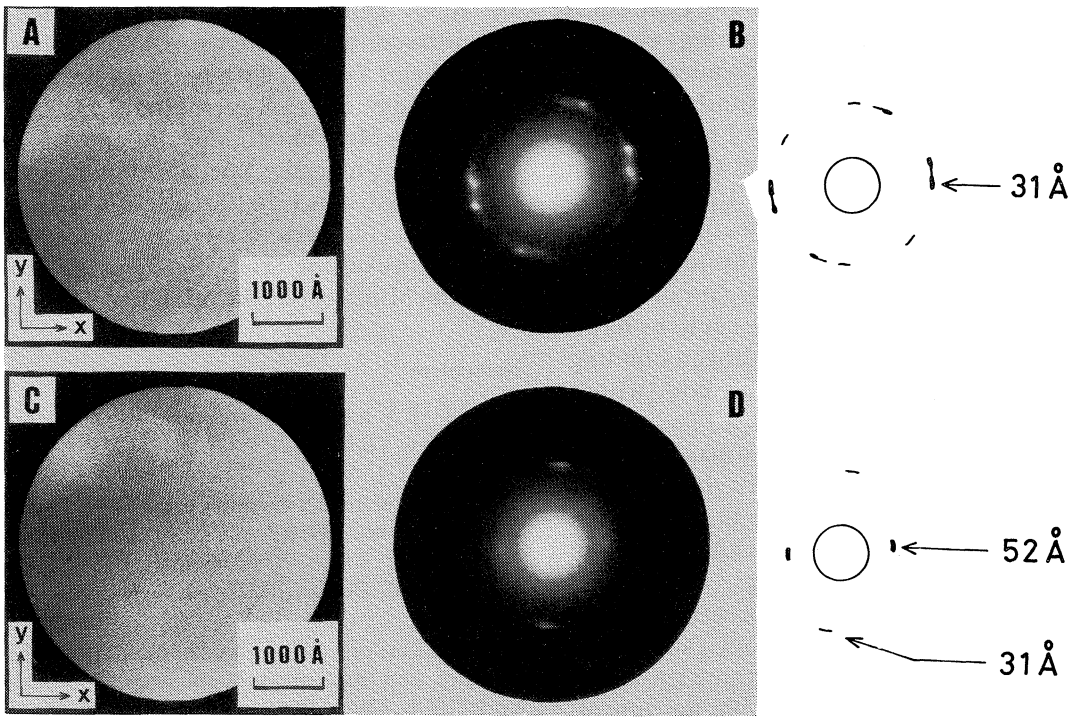

Fig. 8. Electron micrographs for a mixture of (HO)C_5Ala2C_{14} (3.33 mmol dm^{-3}) and Q_2LysC_5Ala2C_{14} (1.67 mmol dm^{-3}) in the aqueous dispersion state at room temperature, as negatively stained with uranyl acetate (A and C); their selected area electron diffraction patterns (B for A and D for C, respectively). Image A and diffraction pattern B were converted into C and D, respectively, by 30° rotation of the specimen around the *y*-axis.

regardless of the sample conditions, sonicated or dispersed. The results apparently indicate that these aggregates do not hold inner aqueous compartments.

A correlation of the r_S value due to DPH embedded in the aggregates with temperature at pH 14 is shown in Fig. 4 (curve B). Apparently, any inflection region is

Table 2. Aggregate Morphology for Synthetic Peptide Lipids in Aqueous Media

Lipid system	Aggregate morphology	N[a]	N'[b]
$(HO)C_5Ala2C_{14}$-$Q_2LysC_5Ala2C_{14}$	H_{II}[c]	2.7[d]	
QC_5Ala2C_n (n=14, 16)	C_{II}[c]	4	
QC_5Ala2C_n-$Q_2LysC_5Ala2C_n$ (n=14, 16)	Bilayer	5.3—6	
$Q_2LysC_5Ala2C_n$ (n=14, 16)	Bilayer	8	
$(Q^{4-})C_5Ala2C_n$ (n=14, 16)[e]	Bilayer		4
$(Q^{4-})_2LysC_5Ala2C_n$ (n=14, 16)[f]	Micelle		8

a) A number of OH groups per molecule. b) A number of O^- groups per molecule. c) Formed above T_m. d) An estimated value from Fig. 5. e) Anionic form of QC_5Ala2C_n. f) Anionic form of $Q_2LysC_5Ala2C_n$.

not observed. This is consistent with the formation of micelles and in good agreement with the result obtained from DSC. The critical aggregate concentration was evaluated from a correlation of the r_S value due to DPH embedded in the aggregate with the lipid concentration; 3.0×10^{-5} mol dm^{-3} for $Q_2LysC_5Ala2C_{16}$ at pH 14. It should be noted that the r_S values for the aggregates formed with $Q_2LysC_5Ala2C_{16}$ at pH 14 are much larger than those for the normal micelles composed of CTAB at various temperatures (Fig. 4, curve C) and comparable to those for the bilayer aggregates of the same lipid in the liquid crystalline state. Thus, this lipid undoubtedly forms rigid micelles in its polyanionic form. We have previously clarified that monocationic peptide amphiphiles having a hydrophobic single-chain segment form rigid cylindrical micelles by means of negative staining electron microscopy, ESR, and low-angle light scattering measurements.[18] We have also observed similar cylindrical micelles in the aqueous dispersion of $N^+C_5Ala2C_8$, having a double-chain segment shorter than those of the corresponding bilayer-forming lipids, $N^+C_5Ala2C_n$ (n=10—18).[6c] In the latter case, the aggregate morphology is controlled by modifying the v and l_c values but not the a_0 value. The aggregate structures of these various peptide amphiphiles seem to be tightened due to the intermolecular hydrogen-bonding interactions among the amino acid moieties within each aggregate.

Concluding Remarks. It became apparent that a series of synthetic peptide lipids having various numbers of hydroxyl groups in their head moieties, $(HO)C_5Ala2C_n$, QC_5Ala2C_n, and $Q_2LysC_5Ala2C_n$, adopt four kinds of aggregate morphology in aqueous media; H_{II}, C_{II}, bilayer, and micellar phases (Table 2). The difference in aggregate morphology can be well correlated with the critical packing parameter, v/a_0l_c, and the a_0 value is cited as a primary factor for controlling the morphology in the present case. The v/a_0l_c value increases in the order: micelle, bilayer, C_{II}, and H_{II} forming lipids. The a_0 value is reasonably correlated with the average number of hydroxyl groups per lipid molecule involved in the head moieties of the individual or mixed nonionic lipids. Although the polar head moieties of these nonionic lipids in the aggregated state are hydrated to a certain extent, the hydration shells of these moieties become much expanded upon deprotonation of the hydroxyl groups. The a_0 value becomes significantly larger under such conditions, and the aggregate morphology undergoes relevant transformations as a consequence. Recent rapid growth of the membrane mimetic chemistry has yielded a large number of bilayer-forming synthetic lipids. On the other hand, relevant nonbilayer-forming lipids have not been explored up to the present time, even though important aspects of such morphological status in the biomembrane fusion have been emphasized.[2] We believe that the present study provides useful molecular criteria for designing nonbilayer-forming lipids.

We are grateful to Professor Tisato Kajiyama and Dr. Kenji Yamada of Kyushu University for the X-ray diffraction measurements and Professor Toyoki Kunitake of Kyushu University for the use of a freeze-fracture device. We also thank Dr. Yoshitsugu Tomokiyo, Mr. Takeshi Manabe, and Mr. Eiji Tanaka of Kyushu University for their comments and expert technical assistance in the electron diffraction measurements. The present work was supported in part by a Grant-in-Aid for Scientific Research No. 58430016 from the Ministry of Education, Science, and Culture.

References

1) J. H. Fendler, "Membrane Mimetic Chemistry," John Wiley, New York (1982), Chap. 6 and 12.

2) a) A. J. Verkleij, *Biochim. Biophys. Acta*, **779**, 43 (1984), and references cited therein; b) P. J. Quinn and W. P. Williams, *ibid.*, **737**, 223 (1983); c) K. Larsson, K. Fontell, and N. Krog, *Chem. Phys. Lipids*, **27**, 321 (1980); d) P. R. Cullis and B. De Kruijff, *Biochim. Biophys. Acta*, **559**, 399 (1979).

3) C. Tanford, "The Hydrophobic Effect: Formation of Micelles and Biological Membranes," John Wiley, New York (1973), Chap. 12.

4) a) J. N. Israelachvili, S. Marčelja, and R. G. Horn, *Quart. Rev. Biophys.*, **13**, 121 (1980); b) D. J. Mitchell and B. W. Ninham, *J. Chem. Soc., Faraday Trans. 2*, **77**, 601 (1981).

5) For an example of morphological transformation between bilayer and micellar aggregates formed with synthetic lipids, see: J.-H. Fuhrhop, D. Fritsch, B. Tesche, and H. Schmiady, *J. Am. Chem. Soc.*, **106**, 1998 (1984).

6) a) Y. Murakami, A. Nakano, and K. Fukuya, *J. Am. Chem. Soc.*, **102**, 4253 (1980); b) Y. Murakami, A. Nakano, and H. Ikeda, *J. Org. Chem.*, **47**, 2137 (1982); c) Y. Murakami, A.

Nakano, A. Yoshimatsu, K. Uchitomi, and Y. Matsuda, *J. Am. Chem. Soc.*, **104**, 3613 (1984).

7) Y. Murakami, J. Kikuchi, T. Takaki, K. Uchimura, and A. Nakano, *J. Am. Chem. Soc.*, **107**, 2161 (1985).

8) K. Kano and J. H. Fendler, *Biochim. Biophys. Acta*, **509**, 289 (1978).

9) Y. Murakami, A. Nakano, J. Kikuchi, T. Takaki, and K. Uchimura, *Chem. Lett.*, **1983**, 1891.

10) R. Grewe and H. Haendler, *Justus Liebigs Ann. Chem.*, **658**, 113 (1962).

11) Y. Murakami, J. Kikuchi, T. Takaki, and K. Uchimura, *J. Am. Chem. Soc.*, **107**, 3373 (1985).

12) Y. Murakami, J. Kikuchi, T. Takaki, and K. Uchimura, *Bull. Chem. Soc. Jpn.*, **59**, 515 (1986).

13) G. L. Kirk, S. M. Gruner, and D. L. Stein, *Biochemistry*, **23**, 1093 (1984).

14) G. Lindblom, K. Larsson, L. Johansson, K. Fontell, and S. Forsén, *J. Am. Chem. Soc.*, **101**, 5465 (1979); W. Longley and T. J. McIntosh, *Nature (London)*, **303**, 612 (1983); K. Larsson, *ibid.*, **304**, 664 (1983).

15) P. Hirsh, A. Howie, R. B. Nicholson, D. W. Pashley, and M. J. Whelan, "Electron Microscopy of Thin Crystals," 2nd ed, R. E. Krieger, New York (1977), pp. 3—6.

16) Y. Murakami, J. Kikuchi, T. Takaki, and K. Uchimura, *Chem. Lett.*, **1986**, 325.

17) N. R. Clement and J. M. Gould, *Biochemistry*, **20**, 1534 (1981).

18) Y. Murakami, A. Nakano, K. Iwamoto, and A. Yoshimatsu, *Chem. Lett.*, **1979**, 951; Y. Murakami, A. Nakano, K. Iwamoto, and A. Yoshimatsu, *J. Chem. Soc., Perkin Trans. 2*, **1980**, 1809.